Technical Report No. 32-687

Analysis of Solar Panel Effect on Louver Performance

Raymond A. Becker

JET PROPULSION LABORATORY
CALIFORNIA INSTITUTE OF TECHNOLOGY
PASADENA, CALIFORNIA

June 1, 1965

Technical Report No. 32-687

Analysis of Solar Panel Effect on Louver Performance

Raymond A. Becker

J. N. Wilson, *Manager*
Mariner C Development

JET PROPULSION LABORATORY
CALIFORNIA INSTITUTE OF TECHNOLOGY
PASADENA, CALIFORNIA

June 1, 1965

Prepared Under Contract No. NAS 7-100
National Aeronautics & Space Administration

CONTENTS

I. Introduction . . . 1

II. Assumptions . . . 2
Discussion of Assumptions . . . 2

III. Mathematical Formulation . . . 4
A. Part I Louver Analysis (No External Source)— Derivation of Expression for ε_{eff-I} . . . 4
B. Part II Louver Analysis (External Source) . . . 5
1. Determination of View Factors . . . 5
2. Derivation of Expression for ε_{eff-II} . . . 6

IV. Results . . . 8
A. Part I . . . 8
B. Part II . . . 9

V. Conclusions . . . 10

Nomenclature . . . 12

References . . . 12

FIGURES

1. Mathematical representation of louver array . . . 4
2. Mirror image technique for equivalent view factor F_{2-2} . . . 4
3. *Mariner* C configuration . . . 5
4. Solar panel-louver geometry, *Mariner* C . . . 5
5. Construction of the equivalent louver backplate and shadower . . . 6
6. Analytical model of the louvers . . . 6
7. Effective emittance vs. louver blade angle . . . 7
8. Comparison of analytical and empirical results . . . 8
9. Effective emittance vs. louver blade angle . . . 8
10. Power radiated vs. temperature . . . 9
11. Effect on ε_{eff} vs. θ of pegging each louver at its maximum ε_{eff} . . . 10
12. Effect on power radiated vs. temperature of pegging each louver at its maximum ε_{eff} . . . 11

ABSTRACT

26023

The influence which a solar panel exerts on the thermal performance of an array of temperature control louvers is investigated analytically in this Report. Although the analytical results apply specifically to the *Mariner C* configuration, many of the concepts included in the analysis are valid for other spacecraft geometries.

The algebraic equations are formulated and solved yielding results which are presented in graphical form. The solar panel was found to have a significant negative effect on the thermal performance of the louvers, but the *Mariner C* configuration is such that this effect can be minimized. The technique for minimization is also presented.

Author

I. INTRODUCTION

To obtain maximum efficiency and reliability in the operation of a spacecraft, the temperature of electronic and mechanical components must be maintained within specified limits. Thermal control of the spacecraft is said to be passive if component temperatures can be held within these limits by the use of surfaces which exhibit the appropriate emissive and absorptive characteristics. Active control implies an inflight variation of thermal parameters to accommodate a corresponding variation in the thermal environment of the spacecraft, while still maintaining component temperatures within the specified limits.

Because thermally isolating a spacecraft from its solar environment is impossible in a practical sense, current passive temperature control techniques are effective only for a limited variation of solar intensity. As mission objectives become more complex, especially the exploration of the planets, passive techniques become less effective and therefore less feasible. When passive techniques fail, active devices must be employed for temperature control.

The use of movable shutters, or louvers, has become widely accepted as currently the most practical method for active temperature control of spacecraft.

Typically, a bank of louvers is mounted over a high emissivity surface to maximize the range of effective emittance. The louver blades themselves have highly reflective surfaces. When the louver blades are closed, the louvers act as a radiation shield between the high emissivity backplate and space. The backplate "sees" only itself, in this case, and the effective emittance is a minimum. As the louver blades open, the view to space of the backplate progressively increases, thereby increasing the effective emittance. The role of the louvers, therefore, is to vary the effective emittance of the backplate by varying its view factor to space.

Should any body, other than a black body at 0°R, be positioned so as to decrease the view factor of the louver backplate to space, the corresponding effective emittance of the backplate would be impaired to some degree depending on the view factor which this body presents, its temperature, and its surface properties.

The purpose of this Report is to develop a method of analysis to handle a situation of this type, and to specifically apply this analysis to the *Mariner C* spacecraft configuration in which a bank of louvers is located perpendicular to, and directly under, each solar panel. The analysis will be divided into two parts:

1. Part I—Determination of the effective emittance of a bank of louvers with no external source (no solar panel).
2. Part II—Determination of the effective emittance of a bank of louvers with an external source (solar panel).

Although these seem to be separate analyses, the second analysis is in reality dependent upon the first. Furthermore, by preventing immediate combination of the two analyses, the results of the first analysis can be utilized independently of the final analytical results.

II. ASSUMPTIONS

Consistent both for Part I and for Part II (the entire analysis), are the following assumptions:

1. Louver blades (both sides) are specular reflectors.
2. Louver blades (both sides) are perfect reflectors, $\rho = 1$.
3. Louver backplate is gray for energy spectrum involved.
4. Louvers are edge pivoted on plane of backplate.
5. Louver backplate is isothermal.
6. All blades have same angular position relative to backplate.
7. Louver backplate emits and reflects diffusely.
8. Solar panel is a planar, black surface.
9. Radiosity is uniform over each backplate segment between two louver blades.

Discussion of Assumptions

Assumption 1 alone makes the analysis so intractable that assumption 2 becomes necessary to allow a relatively straightforward solution. Both assumptions approximate the real case very closely due to the fact that louver blades have typically very low emissivity surfaces (0.03–0.05 for polished aluminum). Since blade surfaces approach perfect optical smoothness, they tend to be primarily specular reflectors especially for the longer wavelengths (infrared region of the energy spectrum).

Assumptions 1 and 2 eliminate the louver blade as an avenue of energy transfer; it becomes relegated to the role of a planar mirror surface, significant only in the determination of the appropriate view factors.

Assumption 3 permits setting $\alpha = \epsilon$ for the backplate for radiation interchange between solar panel and backplate.

Assumption 4 allows analysis of any one channel independent of the others. (A channel is defined as the three-sided enclosure formed by two adjacent louver blades and the segment of the backplate between them.) For mechanical reasons, the *Mariner* louvers are center-pivoted rather than edge-pivoted. No attempt has been made to compare the thermal performance of edge-pivoted and center-pivoted blades. However, both types behave the same near the full-open position and near the full-closed position.

Assumptions 5 and 6 force all channels to be geometrically similar and thermally similar in the sense that all channels are at the same temperature. These assumptions allow the results of the single channel analysis of Part I to be extrapolated to the entire louver array. A necessary condition for the analysis of Part II is that any given channel be bordered by two parallel mirror surfaces (louver blades). Since the louvers are thermally actuated, a non-uniform temperature distribution would preclude this necessary condition.

To compare assumptions 5 and 6 to the real case, the *Mariner* louver design is used as an example. The primary purpose of the *Mariner* louver arrays is to radiate heat from interior modules of electronics. Since these electronic modules are mounted directly to the louver backplate, and since the louver backplate is relatively thick in order to provide structural support, the uniform temperature assumed corresponds quite closely with the real case.

Each louver blade in the *Mariner* design is actuated by means of a bimetallic spiral torsion spring. All bimetallic elements are identical, and each senses the temperature of the backplate in the area of the louver which it activates. If the backplate is isothermal, each bimetallic element senses the same temperature, resulting in the same angular displacement of each louver blade. Hence, once assumption 5 is made, assumption 6 is automatically valid as a direct result of the *Mariner* design.

The validity of assumption 7 is dependent upon the type of coating used on the louver backplate to obtain the necessary thermal properties. Current *Mariner C* design utilizes PV-100 white paint of low solar absorptance–high IR emittance to maximize louver efficiency and minimize solar absorption. This paint is a dielectric which exhibits diffuse emittance and reflectance characteristics and thereby validates assumption 7 at least for the case in point.

Assumption 8 closely approximates reality. In the *Mariner* configuration, the bottoms of the solar panels are painted with a black paint of emissivity 0.88, but for light weight and high structural strength the solar panels are corrugated. From a thermal point of view, these corrugations effectively raise the emissivity of the panels, thereby contributing to the validity of assumption 8.

Assumption 9 is a standard assumption in simple radiation heat transfer analyses. It permits the use of an average view factor for a surface, where a more rigorous approach would require the solution of an integral equation. The magnitude of the error introduced by this assumption has not been determined for this analysis.

III. MATHEMATICAL FORMULATION

A. Part I Louver Analysis (No External Source) — Derivation of Expression for ε_{eff-I}

The geometry of the louver array is shown in Fig. 1.

Energy from backplate (surface 2) reabsorbed by backplate:

$$q_{2-2} = \sigma A_2 T_2^4 \varepsilon_2 F_{2-2}\alpha_2 + \sigma A_2 T_2^4 \varepsilon_2 F_{2-2}\rho_2 F_{2-2}\alpha_2 + \sigma A_2 T_2^4 \varepsilon_2 F_{2-2}\rho_2 F_{2-2}\rho_2 F_{2-2}\alpha_2 + \cdots$$

But

$$\alpha_2 = \varepsilon_2$$

$$\therefore q_{2-2} = \sigma A_2 T_2^4 \varepsilon_2^2 F_{2-2}(1 + \rho_2 F_{2-2} + \rho_2^2 F_{2-2}^2 + \cdots)$$

$$= \sigma A_2 T_2^4 \varepsilon_2^2 F_{2-2}\left(\frac{1}{1-\rho_2 F_{2-2}}\right) \tag{1}$$

Total energy radiated from surface 2:

$$q_2 = \sigma A_2 T_2^4 \varepsilon_2 \tag{2}$$

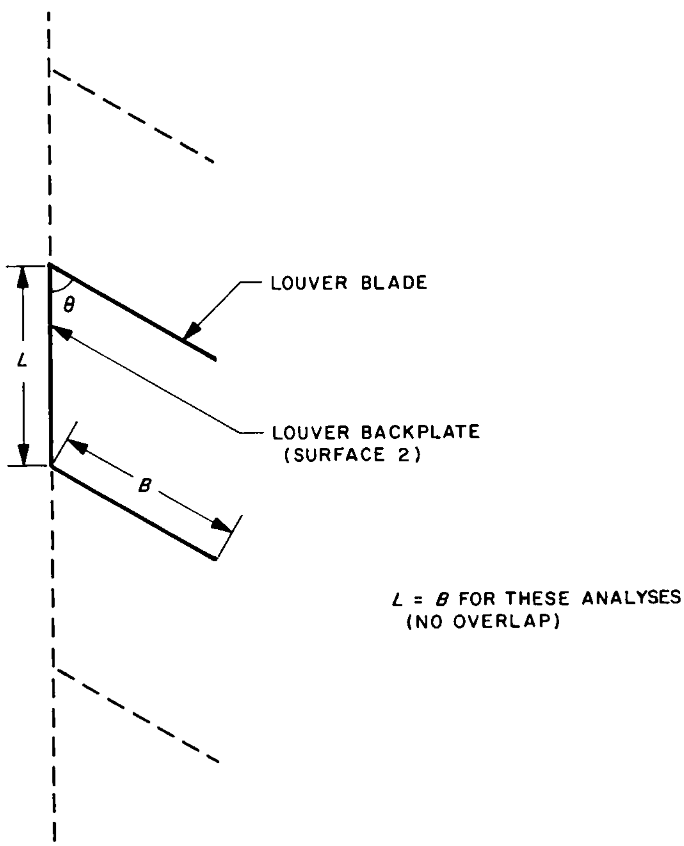

Fig. 1. Mathematical representation of louver array

Energy radiated to space from surface 2:

$$q_{2-s} = q_2 - q_{2-2} = \sigma A_2 T_2^4 \varepsilon_2 - \sigma A_2 T_2^4 \varepsilon_2^2 F_{2-2}\left(\frac{1}{1-\rho_2 F_{2-2}}\right)$$

$$= \sigma A_2 T_2^4 \varepsilon_2\left(1 - \frac{\varepsilon_2 F_{2-2}}{1-\rho_2 F_{2-2}}\right)$$

$$= \sigma A_2 T_2^4 \varepsilon_2\left(\frac{1-F_{2-2}}{1-\rho_2 F_{2-2}}\right) \tag{3}$$

If ε_{eff-I} is defined by the following equation:

$$q_{2-s} = \sigma A_2 T_2^4 \varepsilon_{eff-I}$$

then

$$\varepsilon_{eff-I} = \frac{q_{2-s}}{\sigma A_2 T_2^4} = \varepsilon_2\left(\frac{1-F_{2-2}}{1-\rho_2 F_{2-2}}\right) \tag{4}$$

The accuracy of the analysis now becomes dependent upon the determination of the view factor F_{2-2}. In this case, F_{2-2} is merely the view factor between two flat plates of width 1 intersecting at an angle 2θ where θ is the louver open angle (Fig. 2). A variety of methods are available for this view factor calculation. For the purpose of this Report, view factors were determined both for infinite length louvers and for finite louvers. The former values were determined by mathematical analysis utilizing Hottel's String Rule and the latter values were taken from the Hamilton and Morgan charts (Ref. 1).

Closer scrutiny of Fig. 2 reveals that overlapping of the louver blades ($B > L$) will have no effect on the results of the analysis of Part I.

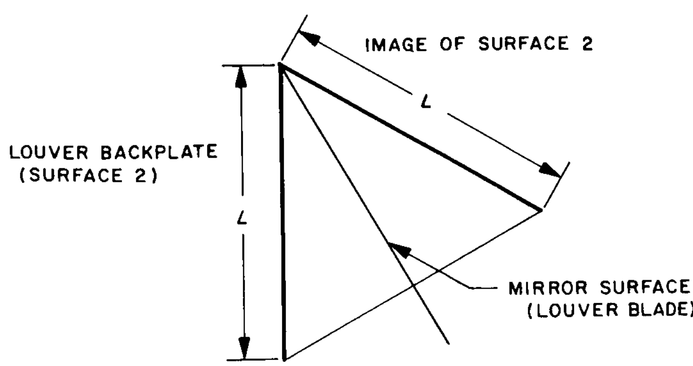

Fig. 2. Mirror image technique for equivalent view factor F_{2-2}

B. *Part II Louver Analysis (External Source)*

1. Determination of View Factors

Although the governing equations and method analysis in this section are valid for an external source of any size, temperature, or geometrical position relative to the louver array, the analysis will be directed toward determining the effect of the solar panel on the thermal parameter ε_{eff} of the adjacent array of louvers in the *Mariner C* configuration.

Briefly describing this configuration, the louver array is mounted on a plane perpendicular to the solar panel plane when the panel is in the extended, or flight, position. The entire configuration is symmetrical about a plane perpendicular to the solar panel and including the longitudinal centerline of the solar panel (Fig. 3).

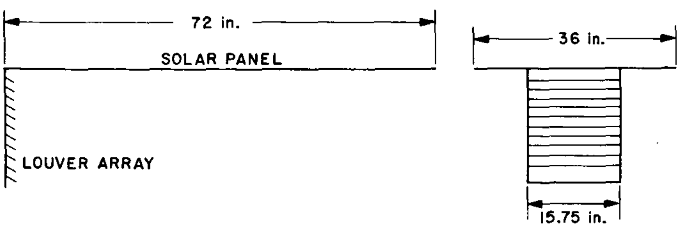

Fig. 3. *Mariner* C configuration

By mirror image techniques, an equivalent backplate area for view factor calculations can be generated that will account for the specular reflectance property of the louver blade surfaces (Ref. 2).

The term "equivalent backplate area" is meant to denote a mathematical plane surface of dimensions and geometrical orientation such that the amount of solar panel radiation incident upon it is equal to the amount which is incident upon that portion of louver backplate which this imaginary plane represents.

For the specific configuration under investigation, the solar panel cannot see the bottom surface of any louver blade directly. Therefore, any solar panel radiation which reaches the louver backplate must arrive by one of three avenues: (1) direct from the solar panel; (2) single reflection from the bottom louver blade of the channel; (3) or multiple reflections between the two louver blades enclosing the channel, the first reflection being from the bottom blade.

At first glance, it would appear that an equivalent surface could be constructed from blade tip to blade tip, but

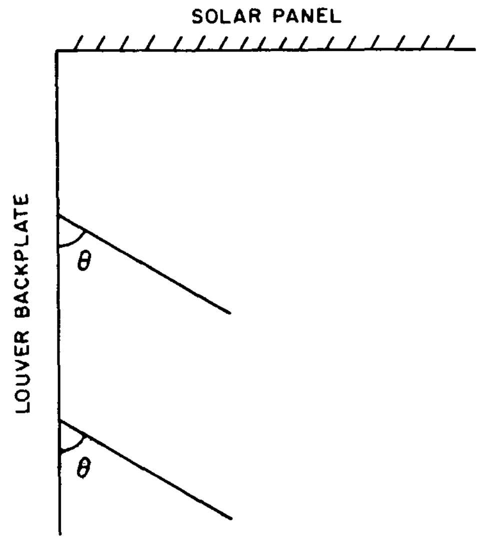

Fig. 4. Solar panel-louver geometry, *Mariner* C

by closer investigation it can be seen that all reflections from the lower blade do not necessarily proceed on to the louver backplate. At this point, note that all solar panel radiation whose angle of incidence on the lower blade is such that it strikes the upper blade will ultimately reach the louver backplate. This stems directly from the geometry of the problem; that is, two parallel mirror surfaces (Fig. 4). If the lower blade is treated as a mirror and the mirror image of the upper blade and louver backplate as seen by the solar panel is constructed, the result is an enclosure shaped like a letter "M" (Fig. 5a). Constructing a planar cover across the feet of the "M" (Fig. 5b) provides the equivalent louver backplate surface to be used in view factor calculations.

One further refinement must be made. An examination of Fig. 5c shows that radiation from far out on the solar panel will reach the equivalent louver backplate when in reality it should fall into the next lower channel. This is corrected by constructing a shadower as in Fig. 5d. This shadower has an effect only at louver open angles (θ) above about 40 deg, but it becomes more and more critical as θ increases toward 90 deg. Figure 6 describes the appropriate trigonometric equations for the determination of the equivalent backplate area and orientation as functions of louver open angle θ, louver spacing L, and louver number C, for no blade overlap, $B = L$.

The equivalent louver backplate shall be designated as surface $2eq$ in the following derivation of the expression for ε_{eff-II}.

The use of mirror image techniques has resulted in the construction of an equivalent backplate surface and a

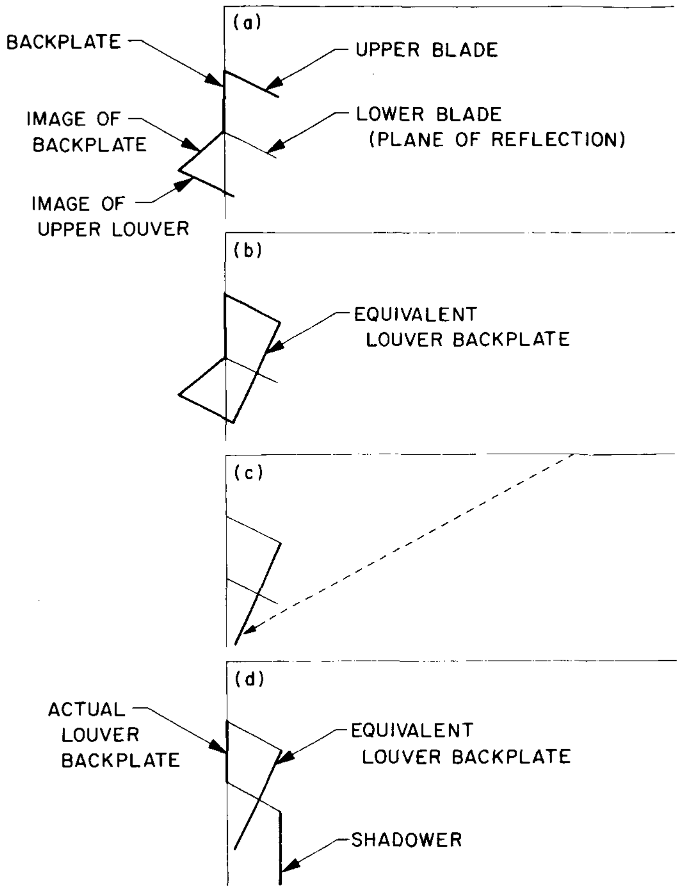

Fig. 5. Construction of the equivalent louver backplate and shadower

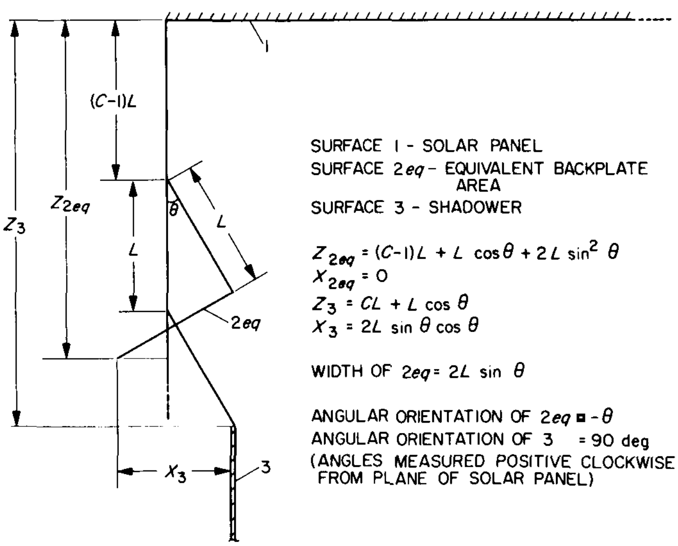

Fig. 6. Analytical model of the louvers

shadower. These fictitious surfaces are used for appropriate view factor determinations, but cannot be used for the subsequent heat transfer calculations. These are accomplished by determining the total solar panel input to each louver channel and combining it with the total louver channel output to obtain the net effect as a function of louver channel position.

2. Derivation of Expression for ε_{eff-II}

In the derivation of the expression for ε_{eff-II}, surface 1 = solar panel; surface 2 = louver backplate (single channel); and surface $2eq$ = equivalent louver backplate (single channel).

The equivalent louver backplate is only for view factor calculations to determine the amount of radiation incident upon the actual louver backplate. Heat transfer from the louver array must be handled as in Part I.

I = radiation from solar panel ultimately absorbed by louver backplate (single channel)

$$\begin{aligned} I &= \sigma A_1 T_1^4 F_{1-2eq}\alpha_2 + \sigma A_1 T_1^4 F_{1-2eq}\rho_2 F_{2-2}\alpha_2 \\ &\quad + \sigma A_1 T_1^4 F_{1-2eq}\rho_2 F_{2-2}\rho_2 F_{2-2}\alpha_2 + \cdots \\ &= \sigma A_1 T_1^4 F_{1-2eq}\alpha_2 (1 + \rho_2 F_{2-2} + \rho_2^2 F_{2-2}^2 + \cdots) \\ &= \sigma A_1 T_1^4 F_{1-2eq}\alpha_2 \left(\frac{1}{1-\rho_2 F_{2-2}}\right) \end{aligned} \tag{5}$$

By definition

$$\varepsilon_{eff} = \frac{P_{net}}{\sigma A_2 T_2^4}$$

Where

P_{net} = net power radiated from louver backplate (single channel)

A_2 = area of louver backplate (single channel)

T_2 = temperature of louver backplate

$$P_{net} = \sigma A_2 T_2^4 \varepsilon_{eff-I} - I \tag{6}$$

$$\begin{aligned} \therefore \varepsilon_{eff-II} &= \frac{\sigma A_2 T_2^4 \varepsilon_{eff-I} - I}{\sigma A_2 T_2^4} \\ &= \varepsilon_{eff-I} - \frac{I}{\sigma A_2 T_2^4} \\ &= \varepsilon_2 \left(\frac{1 - F_{2-2}}{1-\rho_2 F_{2-2}}\right) - \frac{\sigma A_1 T_1^4 F_{1-2eq}\alpha_2}{\sigma A_2 T_2^4}\left(\frac{1}{1-\rho_2 F_{2-2}}\right) \end{aligned} \tag{7}$$

For the usual case, $\varepsilon_2 = \alpha_2$ and $F_{2\text{-}2} = 1 - \sin\theta$ since infinite louver width is a good approximation.

Further,

$$A_1 F_{1\text{-}2eq} = A_{2eq} F_{2eq\text{-}1}$$

and

$$A_{2eq} = 2A_2 \sin\theta$$

Using all these in Eq. (7) gives

$$\varepsilon_{eff\text{-}II} = \frac{\varepsilon_2 \sin\theta}{\varepsilon_2 + \rho_2 \sin\theta}\left[1 - 2F_{2eq\text{-}1}\left(\frac{T_1^4}{T_2^4}\right)\right] \qquad (8)$$

For the case of an infinitely large solar panel at the same temperature as the backplate, Eq. (8) gives the correct result, $\varepsilon_{eff\text{-}II} = \varepsilon_2/2$, for $\theta = 90$ deg.

View factors $F_{2\text{-}2}$ are determined for the *Mariner C* configuration from Hamilton and Morgan view factor charts. As shown in Fig. 7 (Results, Part I), the assumption of infinite length louver blades does not contribute any significant error to the determination of $F_{2\text{-}2}$.

The General Dynamics/Astronautics Radiation Configuration Factors Program was utilized for determination of the view factors $F_{1\text{-}2eq}$ (Ref. 3). This program employs the finite difference approach and allows for shadowing surfaces, a necessary part of this analysis.

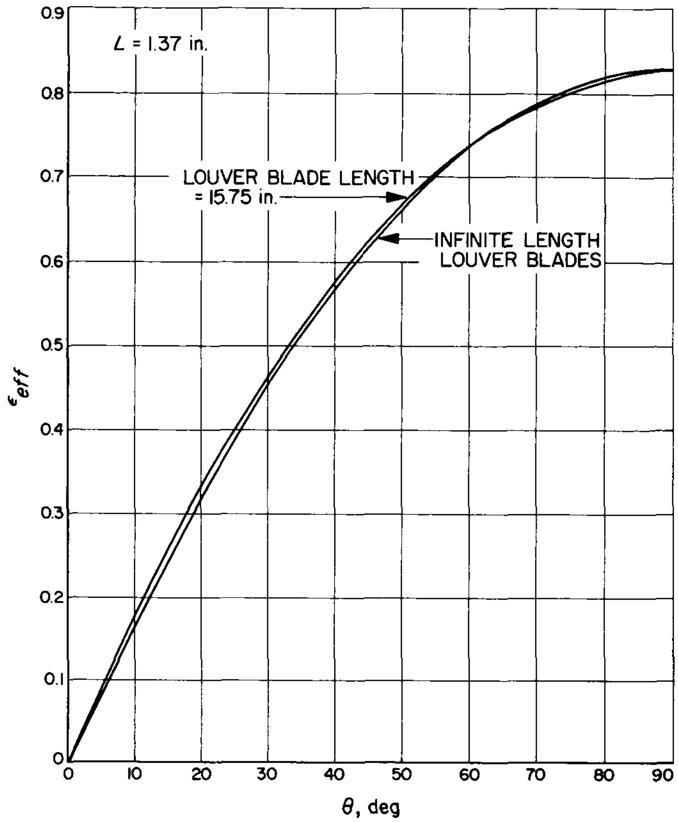

Fig. 7. Effective emittance vs. louver blade angle

IV. RESULTS

A. Part I

The purpose of this part of the analysis was primarily to determine the thermal performance characteristics of a typical *Mariner C* louver array with no external source. For all practical purposes, these characteristics can be described in terms of the thermal parameter ϵ_{eff-I} vs. the geometrical parameter θ. Figure 7 shows the results for both finite and infinite length louvers. It should be kept in mind that the results of Part I are only applicable to a louver array which can see nothing but black space.

Figure 8(a) compares the analytical results to experimental results. It is important to note that the experimental results do not reflect the thermal performance of the *Mariner C* louver array alone, but of the entire louver assembly which includes associated bracketry for structural integrity, louver actuation, and prevention of peripheral leaks. Recognizing this fact, the difference between the two plots can easily be explained.

In the closed position ($\theta = 0$) end clearances on the louver blades allow leakage and are thermally equivalent to black crevices. Since the emissivity of these black crevices is so much higher than the effective emittance of the louver array at $\theta = 0$, these crevices, although of relatively small area, would have a significant effect on the effective emissivity of the entire assembly. As the louvers open, it would be expected that this effect would diminish because the black crevices diminish in area and the theoretical effective emittance increases.

The bracketry effect on the thermal performance of the louvers can be predicted if the bracketry is thought of as a constant area of low emittance. The bracketry effect would be expected to be predominant at large θ since the effective emittance of the array is high. The bracketry has no effect at $\theta = 0$, because its emittance is the same as that of the louver blades.

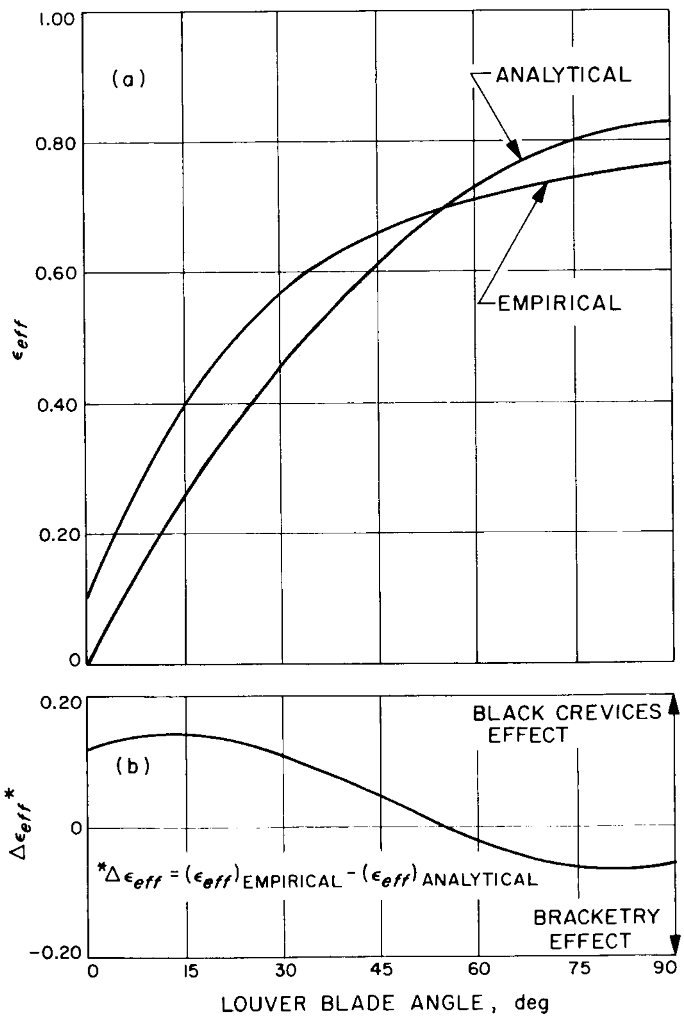

Fig. 8. Comparison of analytical and empirical results

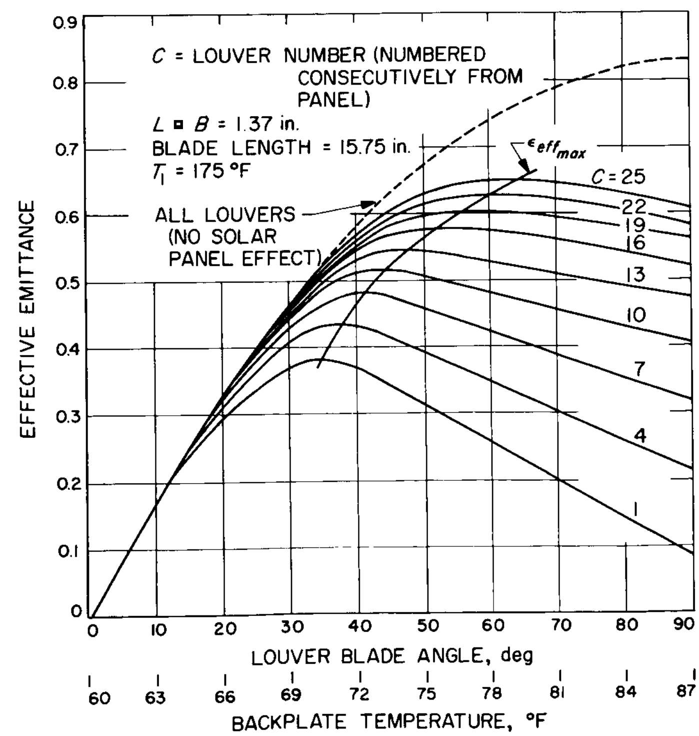

Fig. 9. Effective emittance vs. louver blade angle

These conclusions are presented graphically in Fig. 8(b). The black crevices are the predominant factor at low values of θ, whereas the bracketry effect is predominant at high values of θ.

B. Part II

Results of the analysis including the effect of the solar panel are presented in graphical form in Fig. 9 and 10. Figure 9 presents the $\varepsilon_{eff\text{-}II}$ vs. θ relationship for every fourth louver channel of the *Mariner C* configuration numbered consecutively from the solar panel. Figure 10 merely converts the information of Fig. 9 into a Temperature vs. Power plot for louvers initially opening at 60°F and opening linearly with temperature to full open at 87°F.[1]

[1] Solar panel temperature was considered uniform at 175°F. The results described in this part require that $B = L$ (no blade overlap).

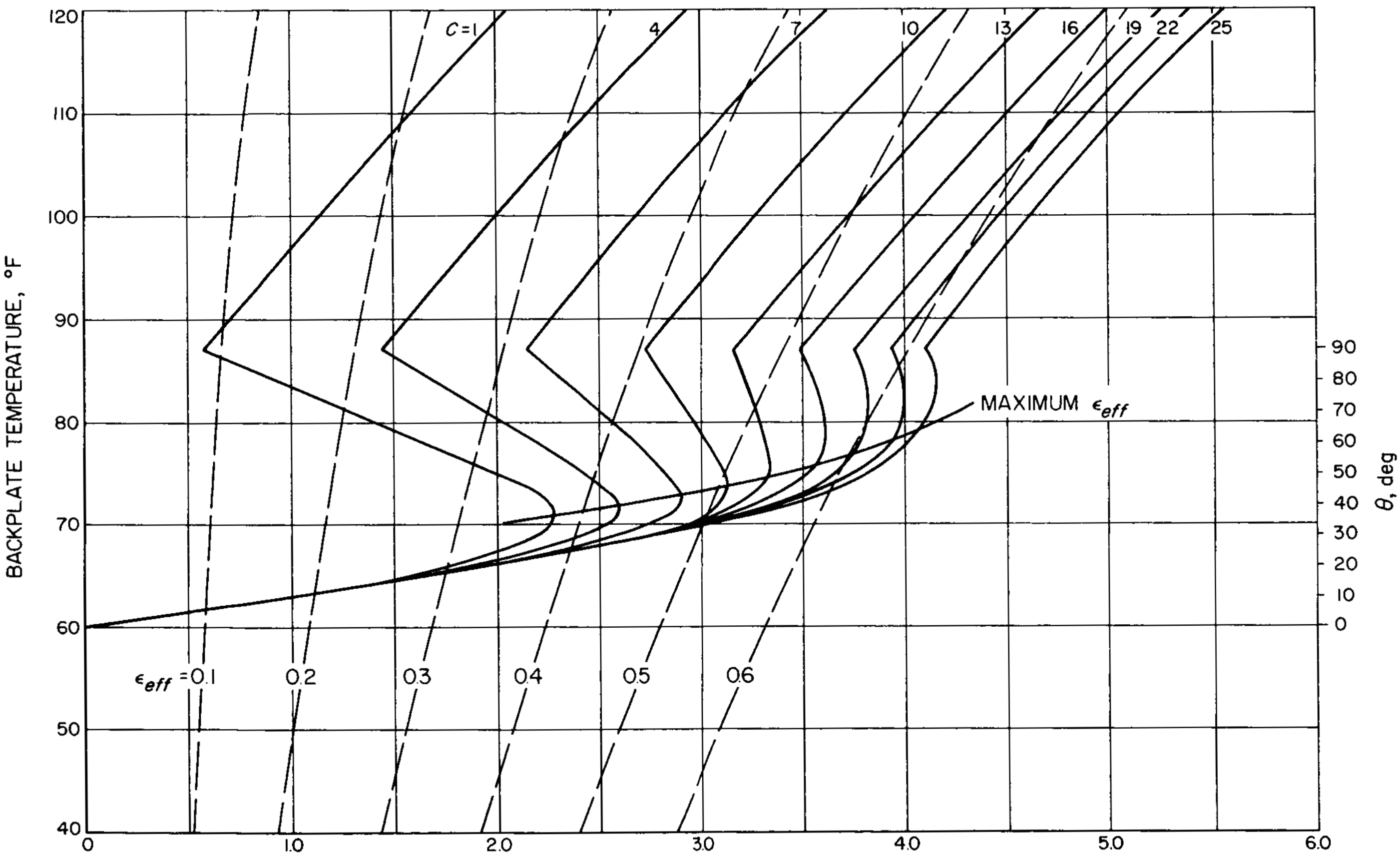

Fig. 10. Power radiated vs. temperature

V. CONCLUSIONS

Several conclusions can be drawn from the solar panel–louver analysis. First of all, it is obvious that for maximum louver efficiency, the louvers must be mounted such that they see nothing but black space. When this "ideal" configuration becomes impractical, the efficiency of the louver array decreases; the extent of this decrease being dependent upon the degree to which any obstructions may impair the view to space of the louver array and the thermal properties of these obstructions.

The *Mariner C* louver–solar panel configuration demonstrates quite effectively the significance of an input to the louver array from an external infrared source.

As shown in Fig. 9, the effective emissivity for each louver channel investigated is maximum at a value of θ less than 90 deg. In Fig. 10 each louver channel has a point of maximum power dissipation within the actuation range ($60°\text{F} < T_2 < 87°\text{F}$). The values of θ corresponding to $\varepsilon_{eff\text{-}max}$ and P_{max} for any given louver channel are not necessarily identical. These two values of θ are distinct for all louvers whose effective emissivity does not peak sharply, that is, louvers 13–25 as determined by this investigation.

If the slope of the ε_{eff} vs. θ plot is only slightly negative over a relatively wide range of θ, as is the case for the more distant louvers, the temperature increase corresponding to the θ increase overcomes the effect of the decreasing ε_{eff}, thereby allowing a positive improvement in power dissipation even though ε_{eff} is decreasing. This effect can be noticed by comparing values of θ corresponding to $\varepsilon_{eff\text{-}max}$ and P_{max} in Fig. 9 and 10 for each of the more distant louvers (13–25). This effect is pointed out to the reader merely as a detail of academic interest. From the standpoint of louver efficiency, the power dissipation capability gained by considering this effect is negligible. For all intents and purposes θ corresponding to $\varepsilon_{eff\text{-}max}$ and θ corresponding to P_{max} for any given louver can be considered identical and shall be in the remainder of this Report.

It is both interesting and significant to note that beyond the point of maximum power dissipation (within the actuation range) the louvers become unstable, dissipating the required power but at the expense of an intolerable increase in temperature, especially for the louvers nearest the solar panel. Fortunately, the *Mariner C* configuration permits a partial, yet acceptable solution to the problem.

By pegging each louver so that it can open no farther than the value of θ corresponding to its point of maximum effective emissivity, the response of the louver remains stable and the characteristic plots are altered as shown in Fig. 11 and 12. For the *Mariner C* configuration, pegging the louvers at the appropriate open angle provides a power dissipation capability of approximately 36.2 watts at 87°F for the entire array. If the louvers are not pegged and allowed to open to 90 deg, the power dissipation capability at 87°F drops to approximately 25.25 watts. Pegging all the louvers at a nominal value of θ equal to 45 deg, the power dissipation capability at 87°F is approximately 33.1 watts. Therefore, pegging the louvers at the appropriate angles provides approximately a 44% improvement in maximum power dissipation capability over the unpegged condition and pegging all louvers at 45 deg provides approximately a 32% improvement.

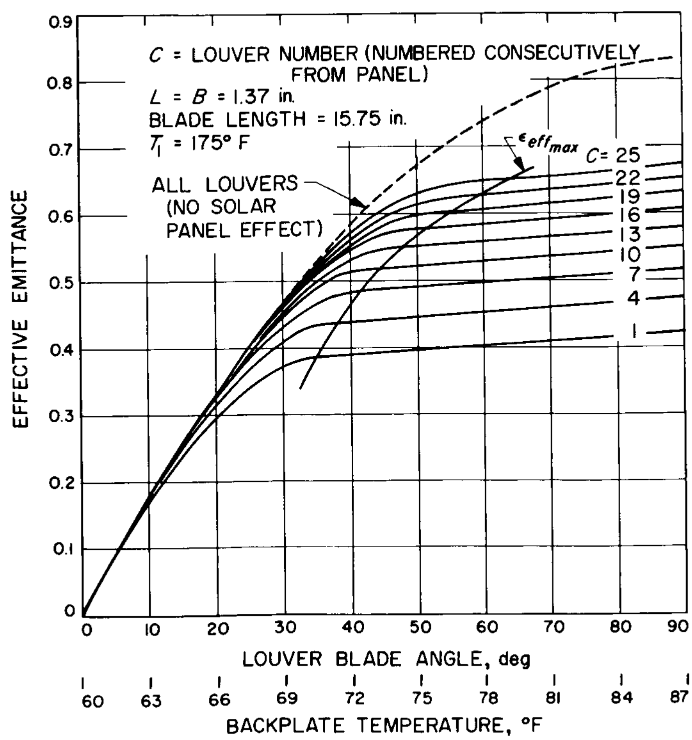

Fig. 11. Effect on ε_{eff} vs. θ of pegging each louver at its maximum ε_{eff}

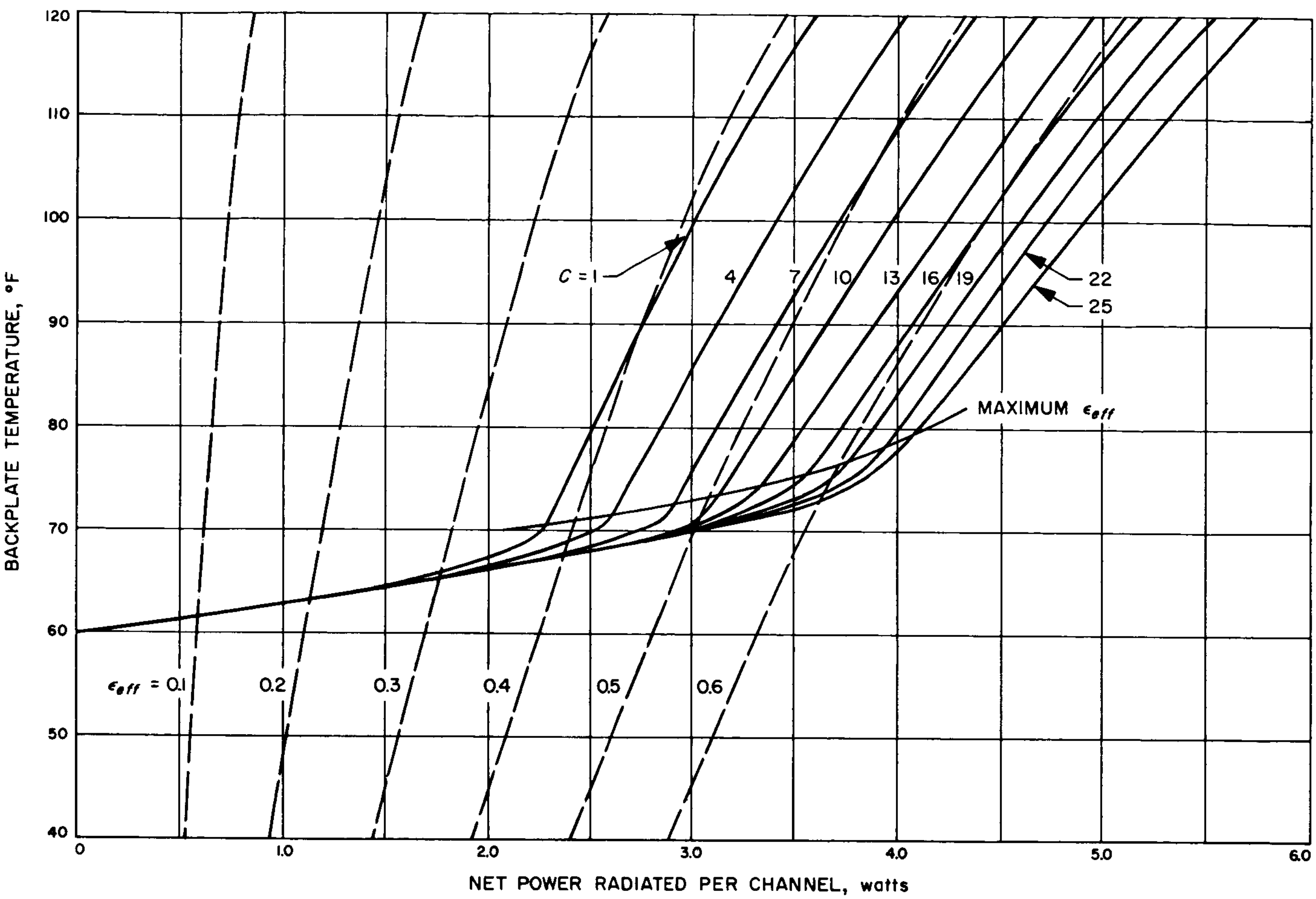

Fig. 12. Effect on power radiated vs. temperature of pegging each louver at its maximum ε_{eff}

As shown in Fig. 10, when a louver reaches the full open position at 87°F, any additional temperature increase improves the effective emissivity. This is due to the fact that the effective emissivity is a function not only of θ but also of the backplate temperature, T_2 (Eq. 8). For a constant value of θ and a given louver, $\varepsilon_{eff\text{-}II}$ will improve with increasing temperature above 87°F because of the fact that the solar panel input I is constant and the higher the temperature the smaller I becomes as a percentage of total power dissipated.

Therefore only if $P_{tot} >> I$ can the solar panel input be neglected and the effective emissivity of all louvers approach the true emissivity of the louver backplate. An equivalent way of stating this condition is $T_2 >> T_1$.

NOMENCLATURE

A area

B louver blade width

C louver blade number (numbered consecutively from solar panel)

F geometric view factor

I total radiation flux from solar panel ultimately absorbed by louver channel

L louver blade spacing

P_{net} net power radiated from louver channel

P_{tot} total power radiated from louver channel

q heat flow rate

T temperature

Subscript s denotes black space at 0°R

Subscript 1 denotes solar panel

Subscript 2 denotes actual louver backplate

Subscript $2eq$ denotes equivalent louver backplate

Subscript 3 denotes shadowing surface

α absorptivity

ε emissivity

ε_{eff-I} effective emittance of louver backplate for no external radiant heat source

ε_{eff-II} effective emittance of louver backplate for external radiant heat source (i.e. solar panel)

θ louver open angle (measured from plane of backplate)

ρ reflectivity

σ Stefan-Boltzmann constant

REFERENCES

1. Hamilton, D. C., and Morgan, W. R., "Radiant-Interchange Configuration Factors," NACA TN-2836, December 1952.

2. Sparrow, E. M., Eckert, E. R. G., and Jonsson, V. K., "An Enclosure Theory for Radiative Exchange Between Specularly and Diffusely Reflecting Surfaces," *Journal of Heat Transfer—Transactions of ASME*, pp. 294-300, November 1962.

3. Drummer, R. S., and Breckenridge, W. T., "Radiation Configuration Factors Program," Report ERR-AN-224, Space Science Laboratory, General Dynamics/Astronautics.

ACKNOWLEDGMENT

The author acknowledges the assistance of the *Mariner* Temperature Control Group and Dave Miller in particular for suggestions and for information about the *Mariner* louvers.